



# Dispersive calculation of complex Regge trajectories for the lightest $f_2$ resonances and the $K^*(892)$



J.A. Carrasco<sup>a</sup>, J. Nebreda<sup>a,b</sup>, J.R. Pelaez<sup>a</sup>, A.P. Szczepaniak<sup>c,d,e</sup>

<sup>a</sup> Departamento de Física Teórica II, Universidad Complutense de Madrid, 28040 Madrid, Spain

<sup>b</sup> Yukawa Institute for Theoretical Physics, Kyoto University, 606-8502 Kyoto, Japan

<sup>c</sup> Physics Department, Indiana University, Bloomington, IN 47405, USA

<sup>d</sup> Center for Exploration of Energy and Matter, Indiana University, Bloomington, IN 47403, USA

<sup>e</sup> Thomas Jefferson National Accelerator Facility, Newport News, VA 23606, USA

## ARTICLE INFO

### Article history:

Received 13 April 2015

Received in revised form 22 July 2015

Accepted 6 August 2015

Available online 11 August 2015

Editor: J.-P. Blaizot

## ABSTRACT

We apply a recently developed dispersive formalism to calculate the Regge trajectories of the  $f_2(1270)$ ,  $f_2'(1525)$  and  $K^*(892)$  mesons. Trajectories are calculated, not fitted to a family of resonances. Assuming that these resonances can be treated in the elastic approximation, the only input are the pole position and residue of a resonance. In all three cases, the predicted Regge trajectories are almost real and linear, with slopes in agreement with the universal value of order  $1 \text{ GeV}^{-2}$ . We also show how these results barely change when considering more than two subtractions in the dispersive formalism.

© 2015 The Authors. Published by Elsevier B.V. This is an open access article under the CC BY license (<http://creativecommons.org/licenses/by/4.0/>). Funded by SCOAP<sup>3</sup>.

## 1. Introduction

There is growing evidence for the existence of non-ordinary hadrons that do not follow the quark model, *i.e.* the quark–antiquark–meson or three-quark–baryon classification. Meson Regge trajectories relate resonance spins  $J$  to the square of their masses and for ordinary mesons they are approximately linear. The functional form of a Regge trajectory depends on the underlying dynamics and, for example, the linear trajectory for mesons is consistent with the quark model as it can be explained in terms of a rotating relativistic flux tube that connects the quark with the antiquark. Regge trajectories associated with non-ordinary mesons do not, however, have to be linear. The non-ordinary nature of the lightest scalar meson, the  $f_0(500)$  also referred to as the  $\sigma$ , together with a few other scalars, has been postulated long ago [1]. In the context of the Regge classification, in a recent study of the meson spectrum in [2] it was concluded that the  $\sigma$  meson does not belong to the same set of trajectories that many ordinary mesons do. In [3], it was concluded that the  $\sigma$  can be omitted from the fits to linear  $(J, M^2)$  trajectories because of its large width. The reason is that its width was taken as measure of the uncertainty on its mass and it was found that, when fitting trajectory parameters, its contribution to the overall  $\chi^2$  was insignificant.

In a recent work [4] we developed a formalism based on dispersion relations for the elastic scattering of two particles with identical mass, that, instead of fitting a specific, *e.g.* linear, form to spins and masses of various resonances, enables us to calculate the trajectory using as input the position and the residue of a complex resonance pole in a scattering amplitude. When the method was applied to the  $\rho(770)$  resonance, which appears as a pole in the elastic  $P$ -wave  $\pi\pi$  scattering, the resulting trajectory was found to be, to a good approximation, linear. The resulting slope and intercept are in a good agreement with phenomenological Regge fits. The slope, which is slightly less than  $1 \text{ GeV}^{-2}$ , is expected to be universal for all ordinary trajectories. It is worth noting that in this approach the resonance width is, as it should be, related to the imaginary part of the trajectory and not a source of an uncertainty. The  $\sigma$  meson also appears as a pole in the  $\pi\pi$   $S$ -wave scattering. The position and residue of the pole have recently been accurately determined in [5] using rigorous dispersive formalisms. When the same method was applied to the  $\sigma$  meson, however, we found quite a different trajectory. It has a significantly larger imaginary part and the slope parameter, computed at the physical mass as a derivative of the spin with respect to the mass squared, is more than one order of magnitude smaller than the universal slope. The trajectory is far from linear, instead it is qualitatively similar to a trajectory of a Yukawa potential. We also note that deviation from linearity is not necessarily implied by the large width of the  $\sigma$  since it was also shown in [4] that resonances with large widths

E-mail address: [jrpelaez@fis.ucm.es](mailto:jrpelaez@fis.ucm.es) (J.R. Pelaez).

may belong to linear trajectories. Our findings give further support for the non-ordinary nature of the  $\sigma$ .

Still, one may wonder if the single case of the  $\rho$  meson, where the method agrees with Regge phenomenology, gives sufficient evidence that it can distinguish between ordinary and non-ordinary mesons. In this letter, therefore we show that other ordinary trajectories can be predicted with the same technique, as long as the underlying resonances are almost elastic. For this purpose, we have concentrated on resonances that decay nearly 100% to two mesons. In addition to the  $\rho$  there are two other well-known examples: the  $f_2(1270)$ , whose branching ratio to  $\pi\pi$  is  $84.8_{-1.2}^{+2.4}\%$ , and the  $f_2'(1525)$ , with branching ratio to  $K\bar{K}$  of  $(88.7 \pm 2.2)\%$ . These resonances are well established in the quark model and as we show below, Regge trajectories predicted by our method come out almost real and linear with a slope close to the universal one. There is an additional check on the method that we perform here. In addition, we have extended the formalism to the case when the resonance pole appears in the elastic scattering of two mesons with different mass, and applied it to the case of the  $K^*(892)$  vector resonance, which decays almost exclusively to  $K\pi$ . Once again the resulting Regge trajectory is a conventional one.

Finally, since the formalism used in the case of the  $\rho$  was based on a twice-subtracted dispersion relation, the trajectory had a linear term plus a dispersive integral over the imaginary part. Since the imaginary part of the trajectory is closely related to the decay width, one might wonder if the  $\rho(770)$ ,  $f_2(1270)$ ,  $f_2'(1525)$  and  $K^*(892)$  trajectories come out straight just because their widths are small and we are just using two subtractions. In other words, that for narrow resonances, the straight line behavior is not predicted but it is already built in the twice subtracted formalism. For this reason, in this work, we also consider three subtractions and show that for the ordinary resonances under study the quadratic term comes out negligible.

The paper is organized as follows. In the next section we briefly review the dispersive method and in Section 3 we present the numerical results. In Section 4 we discuss results of the calculation with three subtractions. In Section 5 we briefly discuss the extension to the unequal mass case and present the results for the  $K^*(892)$ . In Section 6 we discuss briefly some crude estimates of the widths of other resonances that are predicted from the calculated Regge trajectories, as well as the caveats and difficulties to apply or extend this formalism to other resonances. Summary and outlook are given in Section 7.

## 2. Dispersive determination of a Regge trajectory from a single pole

The partial wave expansion of the elastic scattering amplitude,  $T(s, t)$ , of two spinless mesons of mass  $m$  is given by

$$T(s, t) = 32K\pi \sum_l (2l+1)t_l(s)P_l(z_s(t)), \quad (1)$$

where  $z_s(t)$  is the  $s$ -channel scattering angle and  $K = 1, 2$  depending on whether the two mesons are distinguishable or not. The partial waves  $t_l(s)$  are normalized according to

$$t_l(s) = e^{i\delta_l(s)} \sin \delta_l(s) / \rho(s), \quad \rho(s) = \frac{2q}{\sqrt{s}} = \sqrt{1 - 4m^2/s}, \quad (2)$$

where  $q^2 = s/4 - m^2$  is the CM momentum and  $\delta_l(s)$  is the phase shift on the real axis. The unitarity condition in the elastic region,

$$\text{Im}t_l(s) = \rho(s)|t_l(s)|^2, \quad (3)$$

is automatically satisfied. When  $t_l(s)$  is continued from the real axis to the entire complex plane, unitarity determines the amplitude discontinuity across the cut on the real axis above  $s = 4m^2$ . It also determines the continuation in  $s$ , at fixed  $l$ , onto the second sheet where resonance poles are located. It follows from Regge theory that the same resonance poles appear when the amplitude is continued into the complex  $l$ -plane [6], leading to,

$$t_l(s) = \frac{\beta(s)}{l - \alpha(s)} + f(l, s), \quad (4)$$

where  $f(l, s)$  is analytical near  $l = \alpha(s)$ . The Regge trajectory  $\alpha(s)$  and residue  $\beta(s)$  satisfy  $\alpha(s^*) = \alpha^*(s)$ ,  $\beta(s^*) = \beta^*(s)$ , in the complex- $s$  plane cut along the real axis for  $s > 4m^2$ . Thus, as long as the pole dominates in Eq. (4), partial wave unitarity, Eq. (3), analytically continued to complex  $l$  implies,

$$\text{Im}\alpha(s) = \rho(s)\beta(s), \quad (5)$$

and determines the analytic continuation of  $\alpha(s)$  to the complex plane [8]. At threshold, partial waves behave as  $t_l(s) \propto q^{2l}$ , so that if the Regge pole dominates the amplitude, we must have  $\beta(s) \propto q^{2\alpha(s)}$ . Moreover, following Eq. (1), the Regge pole contribution to the full amplitude is proportional to  $(2\alpha + 1)P_\alpha(z_s)$ , so that in order to cancel poles of the Legendre function  $P_\alpha(z_s) \propto \Gamma(\alpha + 1/2)$  the residue has to vanish when  $\alpha + 3/2$  is a negative integer, i.e.,

$$\beta(s) = \gamma(s)\hat{s}^{\alpha(s)} / \Gamma(\alpha(s) + 3/2). \quad (6)$$

Here we defined  $\hat{s} = 4q^2/s_0 = (s - 4m^2)/s_0$  and introduced a scale  $s_0$  to have the right dimensions. The so-called reduced residue,  $\gamma(s)$ , is a real analytic function. Hence, on the real axis above threshold, since  $\beta(s)$  is real, the phase of  $\gamma$  is

$$\arg \gamma(s) = -\text{Im}\alpha(s) \log(\hat{s}) + \arg \Gamma(\alpha(s) + 3/2). \quad (7)$$

Consequently, we can write for  $\gamma(s)$  a dispersion relation:

$$\gamma(s) = P(s) \exp \left( c_0 + c's + \frac{s}{\pi} \int_{4m^2}^{\infty} ds' \frac{\arg \gamma(s')}{s'(s' - s)} \right), \quad (8)$$

where  $P(s)$  is an entire function. Note that the behavior at large  $s$  cannot be determined from first principles, but, as we expect linear Regge trajectories for ordinary mesons, we should allow  $\alpha$  to behave as a first order polynomial at large- $s$ . This implies that  $\text{Im}\alpha(s)$  decreases with growing  $s$  and thus it obeys the dispersion relation [6,7]:

$$\alpha(s) = \alpha_0 + \alpha's + \frac{s}{\pi} \int_{4m^2}^{\infty} ds' \frac{\text{Im}\alpha(s')}{s'(s' - s)}. \quad (9)$$

Assuming  $\alpha' \neq 0$ , from unitarity, Eq. (5), in order to match the asymptotic behavior of  $\beta(s)$  and  $\text{Im}\alpha(s)$  it is required that  $c' = \alpha'(\log(\alpha's_0) - 1)$  and that  $P(s)$  can at most be a constant,  $P(s) = \text{const}$ . Therefore, using Eq. (4), we arrive at the following three equations, which define the “constrained Regge-pole” amplitude [8]:

$$\text{Re}\alpha(s) = \alpha_0 + \alpha's + \frac{s}{\pi} PV \int_{4m^2}^{\infty} ds' \frac{\text{Im}\alpha(s')}{s'(s' - s)}, \quad (10)$$

$$\text{Im}\alpha(s) = \frac{\rho(s)b_0\hat{s}^{\alpha_0+\alpha's}}{|\Gamma(\alpha(s) + \frac{3}{2})|} \exp \left( -\alpha's[1 - \log(\alpha's_0)] \right)$$

$$+ \frac{s}{\pi} PV \int_{4m^2}^{\infty} ds' \frac{\text{Im}\alpha(s') \log \frac{s}{s'} + \arg \Gamma\left(\alpha(s') + \frac{3}{2}\right)}{s'(s' - s)}, \quad (11)$$

$$\beta(s) = \frac{b_0 \hat{s}^{\alpha_0 + \alpha' s}}{\Gamma(\alpha(s) + \frac{3}{2})} \exp\left(-\alpha' s [1 - \log(\alpha' s_0)]\right) + \frac{s}{\pi} \int_{4m^2}^{\infty} ds' \frac{\text{Im}\alpha(s') \log \frac{s}{s'} + \arg \Gamma\left(\alpha(s') + \frac{3}{2}\right)}{s'(s' - s)}, \quad (12)$$

where  $PV$  denotes the principal value. For real  $s$ , the last two equations reduce to Eq. (5). The three equations are solved numerically with the free parameters fixed by demanding that the pole on the second sheet of the amplitude in Eq. (4) is at a given location. Thus we will be able to obtain the two independent trajectories corresponding to the  $f_2(1270)$  and  $f_2'(1525)$  resonances from their respective pole parameters. Note that we are not imposing, but just allowing, linear trajectories.

### 3. Numerical results

In principle, the method described in the previous section is suitable for resonances that appear in the elastic scattering amplitude, *i.e.* they only decay to one two-body channel. For simplicity we are also focusing on cases where the two mesons in the scattering state have the same mass. We assume that both the  $f_2(1270)$  and the  $f_2'(1525)$  resonances can be treated as purely elastic and we will use their decay fractions into channels other than  $\pi\pi$  and  $K\bar{K}$ , respectively, as an additional systematic uncertainty in their widths and couplings. In our numerical analysis we fit the pole,  $s_p$ , and residue,  $|g^2|$ , found in the second Riemann sheet of the Regge amplitude. In this amplitude the  $\alpha(s)$  and  $\beta(s)$  are constrained to satisfy the dispersion relations in Eqs. (11) and (12). Thus, the fit determines the parameters  $\alpha_0, \alpha', b_0$  for the trajectory of each resonance. In practice, we minimize the sum of squared differences between the input and output values for the real and imaginary parts of the pole position and for the absolute value of the squared coupling, divided by the square of the corresponding uncertainties. At each step in the minimization procedure a set of  $\alpha_0, \alpha'$  and  $b_0$  parameters is chosen and the system of Eqs. (10) and (11) is solved iteratively. The resulting Regge amplitude for each  $\alpha_0, \alpha'$  and  $b_0$  is then continued to the complex plane, in order to determine the resonance pole in the second Riemann sheet, and the  $\chi^2$  is calculated by comparing this pole to the corresponding input.

#### 3.1. $f_2(1270)$ resonance

In the case of the  $f_2(1270)$  resonance, we use as input the pole obtained from the conformal parameterization of the  $D0$  wave from Ref. [9]. In that work the authors use different parameterizations in different regions of energy and impose a matching condition. Here we will use the parameterization valid in the region where the resonance dominates the scattering amplitude, namely, in the interval  $2m_K \leq s^{1/2} \leq 1420$  MeV. Moreover, we will decrease the width down to 85% of the value found in [9] to account for the inelastic channels. The conformal parameterization results in the pole located at

$$\sqrt{s_{f_2}} = M - i\Gamma/2 = 1267.3_{-0.9}^{+0.8} - i(87 \pm 9) \text{ MeV}$$

and a coupling of

$$|g_{f_2\pi\pi}|^2 = 25 \pm 3 \text{ GeV}^{-2}.$$

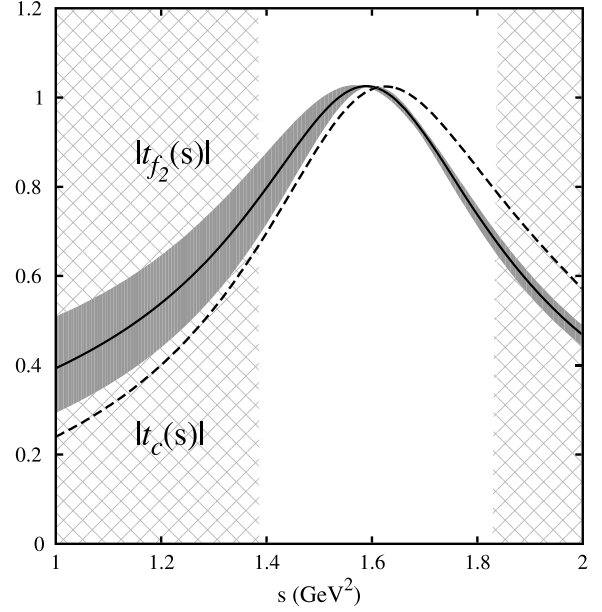


**Fig. 1.** The solid line represents the absolute value of the constrained Regge-pole amplitude for the  $f_2(1270)$  resonance. The gray bands cover the uncertainties due to the errors in the input pole parameters. The dashed line corresponds to the absolute value of the data fit obtained in [9]. Let us recall that only the parameters of the pole given by this parameterization have been used as input, and not the amplitude itself. The regions covered with a mesh correspond to  $s < (M - \Gamma/2)^2$  and  $s > (M + \Gamma/2)^2$ , where the background might not be negligible anymore.

With these input parameters, we follow the minimization procedure as explained above, until we get a Regge pole at  $\sqrt{s_{f_2}} = (1267.3 \pm 0.9) - i(89 \pm 10) \text{ MeV}$  and coupling  $|g_{f_2\pi\pi}|^2 = 25 \pm 3 \text{ GeV}^{-2}$ . In Fig. 1 we show the corresponding constrained Regge-pole amplitude on the real axis versus the conformal parameterization that was constrained by the data [9]. This comparison is a check that our Regge-pole amplitude, which neglects the background  $f(l, s)$  term in Eq. (4), describes well the amplitude in the pole region, namely for  $(M - \Gamma/2)^2 < s < (M + \Gamma/2)^2$ . The gray bands cover the uncertainties arising from the errors of the input and include an additional 15% systematic uncertainty in the width as explained above. Taking into account that only parameters of the pole have been fitted, but not the whole amplitude in the real axis, and that we have completely neglected the background in Eq. (4), the agreement between the two amplitude models is very good, particularly in the resonance region. Of course, the agreement deteriorates as we move away from the peak region as illustrated by the shadowed energy regions  $s < (M - \Gamma/2)^2$  and  $s > (M + \Gamma/2)^2$ .

Since our constrained Regge amplitude provides a good description of the resonance region we can trust the resulting Regge trajectory. The parameters of the trajectory obtained through our minimization procedure are as follows,

$$\alpha_0 = 0.9_{-0.3}^{+0.2}; \quad \alpha' = 0.7_{-0.2}^{+0.3} \text{ GeV}^{-2}; \quad b_0 = 1.3_{-0.8}^{+1.4}. \quad (13)$$

In Fig. 2 we show the real and imaginary parts of  $\alpha(s)$ , with solid and dashed lines, respectively. Again, the gray bands cover the uncertainties coming from the errors in the input pole parameters. We find that the real part of the trajectory is almost linear and much bigger than the imaginary part. It is as expected for Regge trajectories of ordinary mesons. For comparison, we also show, with a dotted line, the Regge trajectory obtained in [2] by fitting a Regge linear trajectory to the meson states associated with  $f_2(1270)$ , which is traditionally referred to as the  $P'$  trajectory. We see that the two trajectories are in good agreement. Indeed,

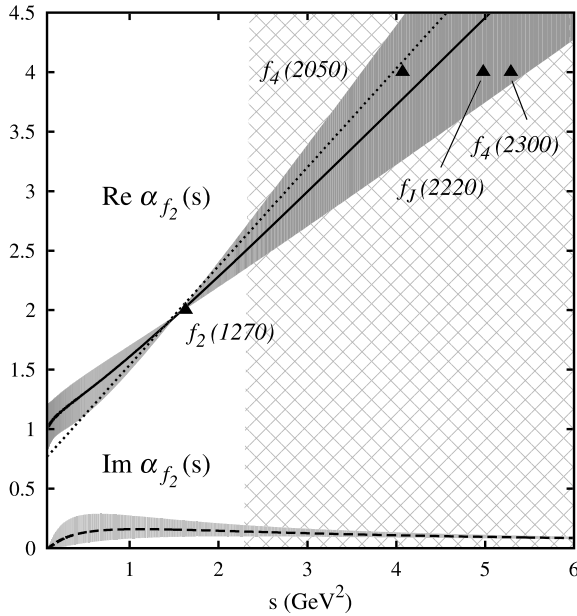


**Fig. 2.** Real (solid) and imaginary (dashed) parts of the  $f_2(1270)$  Regge trajectory. The gray bands cover the uncertainties due to the errors in the input pole parameters. The area covered with a mesh is the mass region starting three half-widths above the resonance mass, where our elastic approach should be considered only as a mere extrapolation. For comparison, we show with a dotted line the  $f_2(1270)$  Regge trajectory obtained in [2], traditionally called the  $P'$  trajectory. We also show the resonances listed in the PDG that are candidates for this trajectory. Note that their average mass does not always coincide with the nominal one, as is the case for the  $f_2(1270)$ .

our parameters are compatible, within errors, with those in [2]:  $\alpha_{P'} \approx 0.71$  and  $\alpha'_{P'} \approx 0.83 \text{ GeV}^{-2}$ . We also include in Fig. 2 the resonances from the PDG [10] listing that could be associated with this trajectory.

In Fig. 2 the trajectory has been extrapolated to high energies, where the elastic approximation does not hold any more and we cannot hope to give a precise prediction for its behavior. The only reason to do this is to show the position of the candidate states connected to the  $f_2(1270)$ . In the figure, this region is covered with a mesh to the right from the line at  $s$  that corresponds to the resonance mass plus three half-widths. Of course, we cannot confirm which of these resonances belongs to the  $f_2(1270)$  trajectory, but we observe that the  $J = 4$  resonance could be the  $f_4(2050)$ , as proposed in [2], or the  $f_J(2220)$ <sup>1</sup> or even the  $f_4(2300)$ . All these resonances appear in the PDG, but are omitted from the summary tables.

### 3.2. $f'_2(1525)$ resonance

As commented above, the  $f'_2(1525)$  decays mainly to two kaons. Although there is no scattering data on the  $l = 2$  elastic  $\bar{K}K$  phase shift in this mass region, the mass and width of the  $f'_2(1525)$  are given in the PDG [10]. Thus we use  $M_{f'_2} = 1525 \pm 5 \text{ MeV}$  and  $\Gamma_{f'_2}^{KK} = 69^{+10}_{-9} \text{ MeV}$ , where the central value of this width corresponds to the decay into  $\bar{K}K$  only. Now, we infer the scattering pole parameters assuming the  $f'_2(1525)$  is well described by an elastic Breit–Wigner shape, so that we take the pole to be at  $s_{f'_2} = (M_{f'_2} - i\Gamma_{f'_2}/2)^2$  and the residue to be  $\text{Res} = -M_{f'_2}^2 \Gamma_{f'_2}^{KK}/2p$ , where  $p$  is the CM momentum of the two

<sup>1</sup> This resonance still “needs confirmation” and it is not yet known whether its spin is 2 or 4 [10].

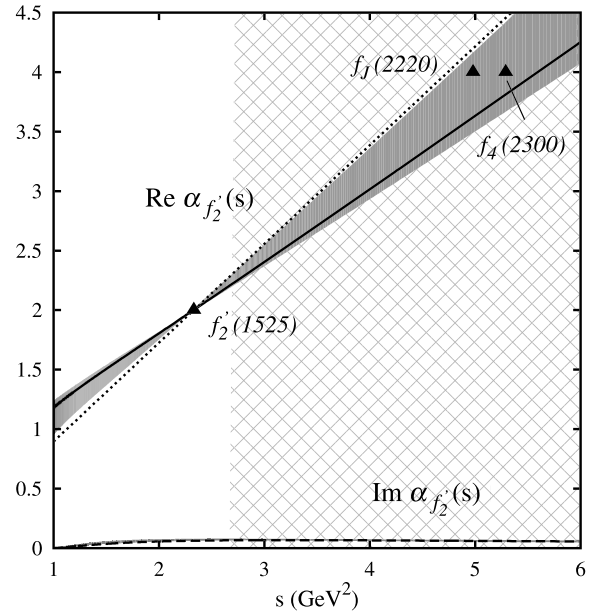


**Fig. 3.** Real (solid) and imaginary (dashed) parts of the  $f'_2(1525)$  Regge trajectory. The gray bands cover the uncertainties due to the errors in the input pole parameters and the area covered with a mesh is the mass region starting three half-widths above the resonance mass, where our elastic approach must be considered just as an extrapolation. For comparison, we show with a dotted line the Regge trajectory obtained in [2] and the resonances listed in the PDG that could belong to this trajectory.

kaons. Since  $|g|^2 = -16\pi(2l+1)\text{Res}/(2p)^{2l}$ , we find  $|g_{f'_2 KK}|^2 = 19 \pm 3 \text{ GeV}^{-2}$ .

With these input parameters we solve the dispersion relations using the same minimization method and obtain the following Regge pole parameters:  $\sqrt{s_{f'_2}} = (1525 \pm 5) - i(34^{+4}_{-5}) \text{ MeV}$  and  $|g_{f'_2 KK}|^2 = 19 \pm 3 \text{ GeV}^{-2}$ . Since we lack experimental data to compare the amplitudes, we proceed to examining the trajectory. The parameters that we obtain are

$$\alpha_0 = 0.53^{+0.10}_{-0.44}; \quad \alpha' = 0.63^{+0.20}_{-0.05} \text{ GeV}^{-2}; \quad b_0 = 1.33^{+0.63}_{-0.09}, \quad (14)$$

which give the Regge trajectory shown in Fig. 3. Again, we find the real part nearly linear and much larger than the imaginary part. As in the case of the  $f_2(1270)$ , the slope is compatible with that found for the  $P'$  trajectory in [2]  $\alpha'_{P'} \approx 0.83 \text{ GeV}^{-2}$ , and the intercepts also agree.

As we did for  $f_2(1270)$ , we include in Fig. 3 the  $J = 4$  candidates for the  $f'_2(1525)$  trajectory. These are the  $f_J(2220)$  and the  $f_4(2300)$ . We remark that there is no experimental evidence of the  $f_4(2150)$  that was predicted in [2] from their analysis of the  $f'_2(1525)$  trajectory. As commented before, these resonances lie in a region, covered with a mesh in Fig. 3, beyond the strict applicability limit of our approach, where our results must be considered qualitatively at most.

Finally, we remark that the PDG list includes another  $f_2$  resonance, albeit requiring confirmation. It has a mass between that of the  $f_2(1270)$  and the  $f'_2(1525)$  and it could also have either the  $f_J(2220)$  or  $f_4(2300)$  as the higher mass partner.

### 4. Dispersion relation with three subtractions

As already mentioned in the introduction, one may wonder whether the linearity of the trajectories we obtain for the two D-wave resonances, as well as for the  $\rho(770)$  in [4], is related to the

**Table 1**  
Parameters of the  $f_2(1270)$ ,  $f_2'(1525)$  and  $\rho(770)$  Regge trajectories using three-time subtracted dispersion relations.

	$\alpha_0$	$\alpha'$ (GeV <sup>-2</sup> )	$\alpha''$ (GeV <sup>-4</sup> )	$b_0$
$f_2(1270)$	1.01	0.97	0.04	2.13
$f_2'(1525)$	0.42	0.65	0.02	4.58
$\rho(770)$	0.56	1.11	0.03	0.88

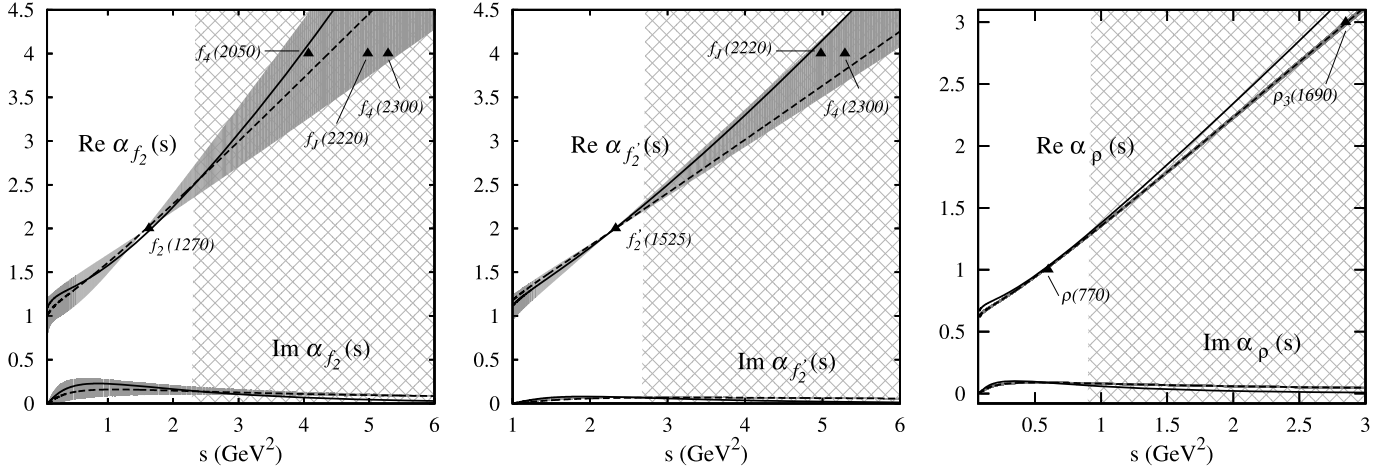


**Fig. 4.** Regge trajectories obtained using three-time subtracted dispersion relations (solid lines) compared to the ones obtained with twice-subtracted dispersion relations (dashed lines with gray error bands).

use of two subtractions in the dispersion relation for  $\alpha(s)$ . In particular, since the resonances are rather narrow one could expect the imaginary part of their trajectories to be small, so that if the last term in Eq. (9) was dropped the trajectory would be reduced to a straight line. Thus, in order to show that the linearity of the trajectory is not forced by the particular parameterization, we repeated the calculations using three subtractions in the dispersion relations,

$$\text{Re } \alpha(s) = \alpha_0 + \alpha' s + \alpha'' s^2 + \frac{s^2}{\pi} PV \int_{4m^2}^{\infty} ds' \frac{\text{Im} \alpha(s')}{s'^2 (s' - s)}, \quad (15)$$

$$\begin{aligned} \text{Im } \alpha(s) = & \frac{\rho(s) b_0 \hat{s}^{\alpha_0 + \alpha' s + \alpha'' s^2}}{|\sqrt{\Gamma(\alpha(s) + \frac{3}{2})}|} \\ & \times \exp \left( -\frac{1}{2} [1 - \log(\alpha'' s_0^2)] s (R + \alpha' s) - Q s \right. \\ & \left. + \frac{s^2}{\pi} PV \int_{4m^2}^{\infty} ds' \frac{\text{Im} \alpha(s') \log \frac{\hat{s}}{s'} + \frac{1}{2} \arg \Gamma \left( \alpha(s') + \frac{3}{2} \right)}{s'^2 (s' - s)} \right), \end{aligned} \quad (16)$$

with

$$R = B - \frac{1}{\pi} \int_{4m^2}^{\infty} ds' \frac{\text{Im} \alpha(s')}{s'^2}, \quad (17)$$

and

$$Q = -\frac{1}{\pi} \int_{4m^2}^{\infty} ds' \frac{-\text{Im} \alpha(s') \log \hat{s}' + \frac{1}{2} \arg \Gamma \left( \alpha(s') + \frac{3}{2} \right)}{s'^2}. \quad (18)$$

The reason why the constants  $R$  and  $Q$  and the square root of  $\Gamma$  have been introduced is to ensure that, at large  $s$ ,  $\text{Im} \alpha(s)$

behaves as  $1/s$ . The parameters that we obtain for the trajectories with these dispersion relations are shown in Table 1.

With the above parameterization we obtain for the fitted pole parameters  $\sqrt{s_{f_2}} = 1267.3 - i90$  MeV,  $|g_{f_2 \pi \pi}|^2 = 25$  GeV<sup>-2</sup>,  $\sqrt{s_{f_2'}}$  = 1525 - i35 MeV,  $|g_{f_2' \pi \pi}|^2 = 19$  GeV<sup>-2</sup>,  $\sqrt{s_{\rho}}$  = 763 - i74 MeV and  $|g_{\rho \pi \pi}|^2 = 35$  GeV<sup>-2</sup>. Therefore, despite having four parameters to fit three numbers, we find no real improvement in the description of the poles. In the case of three subtractions, neglecting the imaginary part of the resonances results in a quadratic trajectory. Therefore, in Fig. 4 we compare the trajectories using the three (solid line) and the two (dashed line) subtractions in the dispersion relations. We observe that in both cases these have a curvature, but that in the elastic region the trajectories are almost linear. The difference between the two methods only becomes apparent for masses well above the range of applicability. Moreover, the difference between the results obtained using two and three subtractions can be used as an indicator of the stability of our results and therefore confirms that the applicability range for our method is well estimated and ends as soon as the inelasticity in the wave becomes sizable.

### 5. The Regge trajectory of the $K^*(892)$

So far we have been dealing with meson resonances whose associated poles appear in the elastic scattering of two particles with identical mass. However, it is relatively straightforward to extend the formalism to the scattering of two mesons with different masses,  $m_1$  and  $m_2$ . The only changes are due to the fact that momenta and energy are related differently when there are two different masses than when the two masses are equal. In particular, the center of mass momentum is now given by  $q^2 = (s - (m_1 + m_2)^2)(s - (m_1 - m_2)^2)/4s$ . Hence, the elastic threshold starts at  $s = (m_1 + m_2)^2$ , which becomes the lower integration limit of the integral equations. In addition, this new expression for  $q^2$  has to be taken into account in the definitions of  $\rho(s)$  and  $\hat{s}$ .

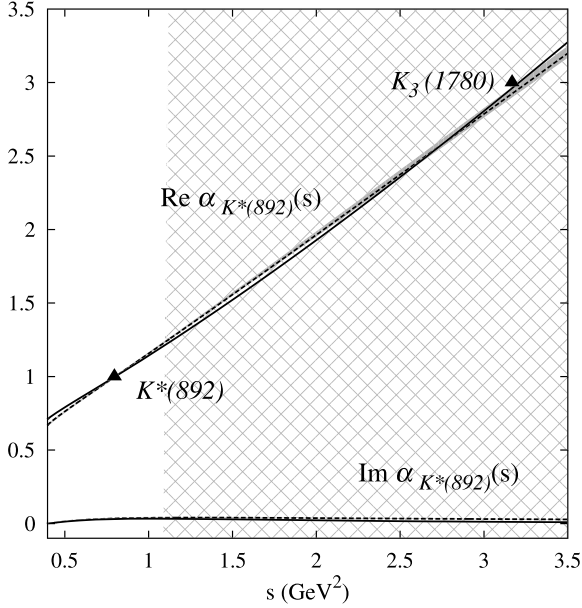


**Fig. 5.** Regge trajectories of the  $K^*(892)$  obtained using two and three-time subtracted dispersion relations, represented as dashed and solid lines, respectively. The mesh region starts at the  $K\eta$  threshold where inelasticity starts becoming important, making our method less reliable.

As an example we will deal with the  $K^*(892)$  vector resonance, which appears in the isospin 1/2 and angular momentum 1 elastic kaon-pion scattering channel with a branching ratio to  $K\pi$  of  $\simeq 100\%$  [10]. Our approach is valid for single channel elastic scattering and thus we need the isospin symmetric formalism, but the charged and neutral  $K^*(892)$  have a slightly different mass. For this reason we have taken as input for the  $K^*(892)$  mass its isospin weighted average and the difference between the charged and neutral states is included in the uncertainty, i.e. we use  $M_{K^*} = 893.7 \pm 2.3$  MeV. Similarly, we use  $\Gamma_{K^*} = 49.4 \pm 2.3$  MeV. The resonance is well approximated by a Breit-Wigner shape near the pole, which gives  $|g_{K^*K\pi}| = 31.3 \pm 1.6$ . We performed both the two- and three-subtracted calculations and in both cases the fitted pole lies almost exactly on top of the input. The resulting parameters for the twice-subtracted case are:

$$\begin{aligned} \alpha_0 &= 0.32 \pm 0.01; & \alpha' &= 0.83 \pm 0.01 \text{ GeV}^{-2}; \\ b_0 &= 0.48 \pm 0.03, \end{aligned} \quad (19)$$

whereas for the three-subtracted case the central values are  $\alpha_0 = 0.41$ ,  $\alpha' = 0.71 \text{ GeV}^{-2}$ ,  $\alpha'' = 0.038 \text{ GeV}^{-4}$  and  $b_0 = 0.57$ . In Fig. 5 we show the resulting trajectories. Note that in this case the two and three subtracted cases are almost indistinguishable. The imaginary part is very small, even more so than in the other cases (consistently with the smaller width) and the real part is almost a straight line. The resulting trajectories are therefore consistent with those for ordinary meson trajectories. Remarkably, the trajectory crosses  $J = \text{Re}\alpha = 3$  at  $\sqrt{s} = 1797 \pm 8$  MeV, thus it predicts a spin 3 resonance with strangeness and isospin 1/2 with such a mass. Recalling once more that our trajectories are not a fit to the mesons, this is remarkably close to the  $K_3^*(1780)$  state, whose mass listed in the PDG is  $M_{K_3^*} = 1776 \pm 7$  MeV.

## 6. Discussion

As we have already remarked, our formalism deals with Regge amplitudes as complex functions  $\alpha(s)$  with a real and an imaginary part. Phenomenological analyses in the literature focus on

the real part, since for ordinary mesons it is much larger than the imaginary part and because the energy at which  $\text{Re}\alpha$  takes an integer value (even or odd depending on the signature of the trajectory) is nothing but the mass of a resonance. We have seen that our approach predicts almost real and straight trajectories for four well-known resonances, consistently with their interpretation as conventional  $\bar{q}q$  mesons. In this sense our approach predicts the existence of further resonances at higher masses on each trajectory. In particular we have seen the appearance of a  $\rho_3$ , two  $f_4$ 's and a  $K_3^*$  as higher spin states on the Regge trajectories of the  $\rho(770)$ ,  $f_2(1270)$ ,  $f_2'(1525)$  and  $K^*(892)$ , respectively. We have also seen that these predicted resonances fall very close to resonances listed in the PDG with those very same quantum numbers. Of course, these predictions have to be interpreted carefully, since these higher spin resonances decay to more than one channel and therefore lie beyond the elastic scattering region of our approach.

However, we are also predicting the imaginary part of the trajectory, consistently with dispersion relations. Moreover, for Breit-Wigner resonances that have just a single dominant decay mode, their width can be related to their Regge trajectory as  $\Gamma = \text{Im}\alpha/[M(\text{Re}\alpha)']$ . Of course, the predicted resonances are not elastic and not necessarily of a Breit-Wigner form. Nevertheless, in view of the good mass predictions that result when extrapolating our calculations into the higher mass/spin region one is tempted to use the previous simple relation between the resonance width and  $\alpha$  to obtain an estimate of their partial width to the scattering channel from which each Regge trajectory was obtained. With all these caveats in mind, we have found that these widths estimates come out fairly reasonable when compared with the existing experimental information. Let us then comment on each one separately:

- For the  $\rho_3(1690)$ , which lies in the  $\rho(770)$  trajectory, the PDG lists 14 decay modes. Of these, the largest branching fraction,  $\sim 71\%$ , is to  $4\pi$ , whereas the branching ratio to  $\pi\pi$  is  $23.6 \pm 1.3\%$ . Unfortunately, although the  $\rho_3(1690)$  mass is very precisely determined to be  $M_{\rho_3}^{\text{exp}} = 1688.8 \pm 2.1$  MeV, the PDG lists many different determinations of the  $\rho_3(1690)$  width, depending on what decay modes are included in the analysis. For example, when considering  $\pi\pi, K\bar{K}$  and  $K\bar{K}\pi$  decays, it is found that  $\Gamma_{3,\text{tot}}^{\text{exp}} = 161 \pm 10$  MeV, but when considering the dominant  $4\pi$  decay mode, the total with it is  $\Gamma_{3,\text{tot}}^{\text{exp}} = 129 \pm 10$  MeV, and the analysis with  $K\bar{K}$  and  $K\bar{K}\pi$  modes yields the largest total width of  $\Gamma_{3,\text{tot}}^{\text{exp}} = 204 \pm 18$  MeV. The last two values basically span the whole range of total widths. Taking into account the branching ratio to  $\pi\pi$  one would then find  $\Gamma_{\rho_3 \rightarrow \pi\pi}^{\text{exp}} = 38 \pm 3$  MeV,  $\Gamma_{\rho_3 \rightarrow \pi\pi}^{\text{exp}} = 30 \pm 3$  MeV and  $\Gamma_{\rho_3 \rightarrow \pi\pi}^{\text{exp}} = 48 \pm 5$  MeV, respectively. From our twice subtracted calculation we obtain  $\Gamma_{\rho_3} = 31.7$  MeV, remarkably consistent with the experimental estimates above. However, we must consider systematic uncertainties in the extrapolation and, for instance within the three-time subtracted formalism we predict 7.1 MeV. In conclusion, our results are reasonably consistent with the experimental results, although they both have rather large uncertainties. It is worth noting that we are estimating that  $\Gamma_{\rho_3 \rightarrow \pi\pi} < \Gamma_{\rho \rightarrow \pi\pi} \simeq 140$  MeV. Even with the present large uncertainties in the PDG, this is definitely the case.
- For the  $f_4(2050)$ , which is the spin 4 resonance that lies closest to our  $f_2(1270)$  trajectory, six decay modes have been seen, according to the PDG. Of these, the largest decay fraction is to  $\pi\pi$ , but it is only  $(17.5 \pm 1.5)\%$ . According to the PDG, the total width is  $\Gamma_{\rho_4,\text{tot}}^{\text{exp}} = 237 \pm 18$  MeV. Thus we estimate  $\Gamma_{\rho_4 \rightarrow \pi\pi}^{\text{exp}} = 40 \pm 5$  MeV.

This experimental value can be compared with our twice-subtracted formalism, which in this case comes too large,  $\Gamma_{\rho_4 \rightarrow \pi\pi} = 72.9$  MeV. However, the three subtracted formalism yields  $\Gamma_{\rho_4 \rightarrow \pi\pi} = 40.3$  MeV, right on top the experimental value. Thus our predictions are qualitatively consistent with observations, although with large uncertainties. Once again, we remark that our approach predicts  $\Gamma_{f_4 \rightarrow \pi\pi} < \Gamma_{f_2 \rightarrow \pi\pi} \simeq 185$  MeV, in good agreement with observations.

- In Fig. 4 we have already seen that two resonances fall within the area enclosed between our twice subtracted and tree-times subtracted  $f_2'(1525)$  trajectories. The twice-subtracted curve would prefer the  $f_4(2300)$  for which the PDG estimates  $\Gamma_{f_4, tot}^{exp} = 250 \pm 80$  MeV. This resonance is not well established and is omitted from the summary tables. Six modes have been seen, including  $K\bar{K}$ , but their branching fractions are not given. Our crude elastic estimate would be  $\Gamma_{f_4 \rightarrow K\bar{K}} = 34$  MeV. In contrast the three-time subtracted formalism would prefer the  $f_J(2220)$ , in case its spin was 4 (it is still undetermined whether it is 2 or 4). Its total width in the PDG is  $\Gamma_{f_J, tot}^{exp} = 23_{-7}^{+8}$  MeV, but no branching fraction to  $K\bar{K}$  is provided and we cannot deduce the partial decay width to  $K\bar{K}$ . The crude estimate of the three-time subtracted formalism is  $\Gamma_{f_J \rightarrow K\bar{K}} = 13.2$  MeV.

Once again, note that our approach predicts for this resonance  $\Gamma_{f_4 \rightarrow K\bar{K}} < \Gamma_{f_2(1525) \rightarrow K\bar{K}} \simeq 73$  MeV, irrespective of whether we make two or three subtractions.

- Finally, a  $K_3^*$  appears as the second state in our prediction for the Regge trajectory of the  $K^*(892)$ . As we have seen, this is very close to the  $K_3^*(1780)$ , for which the PDG estimates a total width of  $159 \pm 21$  MeV and lists five decay channels. Four of them have branching fractions between 19 and 30%, so that once again the decay regime of this resonance is very inelastic. In particular, the branching fraction to  $K\pi$  is  $18.8 \pm 1.0\%$  so that the partial width can be estimated as  $\Gamma_{K_3^* \rightarrow K\pi}^{exp} = 29.9 \pm 4.3$  MeV.

Our elastic estimate would be  $\Gamma_{K_3^* \rightarrow K\pi} = 20$  MeV with two subtractions and 7.3 MeV with three. Thus, fairly reasonable within the large uncertainties of our extrapolation and the caveats of using an elastic formalism. Note that, once more, our formalism correctly predicts  $\Gamma_{K_3^* \rightarrow K\pi} < \Gamma_{K^*(892) \rightarrow K\pi} \simeq 50$  MeV, which is indeed consistent with observations.

Even though the high spin states on each trajectory decay to many different channels and an inelastic formalism is called for, our crude estimates as extrapolations of the elastic formalism with the use of the elastic Breit–Wigner pole parameterization yield partial widths to the channel under study that are qualitatively consistent with observations. Remarkably, our approach always finds that the decay width to the channel under study is smaller for the second resonance in the Regge trajectory than for the first one.

At this point, being able to calculate the  $\rho(770)$  and  $f_2(1270)$  trajectories, one might wonder if one could cover with the same formalism the remaining leading  $\bar{q}q$ -Regge trajectories and describe those of the  $\omega(782)$  and  $a_2(1320)$ . This would require an extension for the two-body unitarity to the three-body case since the main decay mode of these states is to three pions (the branching fractions are  $\sim 90\%$  and  $\sim 70\%$  respectively). When the three body state is dominated by narrow, two body resonances, e.g.  $\rho\pi$ , the three-body unitarity relation can be approximated by a quasi two-body one. Even in this case, however, the present formalism cannot be directly applied since the quasi-two body phase space has different analytical properties compared to the one for two stable particles. In addition, in the case of the  $a_2(1320)$  it has

several significant decay modes ( $\eta\pi$ ,  $\omega\pi\pi$  and  $K\bar{K}$  add up to a 30% branching fraction), so that, not only a three body approach, but also an inelastic one should be considered from the very beginning. Thus the formalism used in this work is not suitable to calculate the  $\omega(782)$  and  $a_2(1320)$  trajectories. We think an extension of the framework to the coupled two-body (or quasi-two body system) can be formulated using the N-over-D matrix methods, but this lies well beyond the scope of this work.

## 7. Summary and outlook

In [4] a dispersive method was developed to calculate Regge trajectories of resonances that appear in the elastic scattering of two mesons. We showed how, using the associated scattering pole of the resonance it is possible to determine whether its trajectory is of a standard type, i.e. real and linear as followed by “ordinary”  $\bar{q}q$ -mesons, or not. This method thus provides a possible benchmark for identifying non-ordinary mesons. In particular the ordinary Regge trajectory of the  $\rho(770)$ , which is a well-established  $\bar{q}q$  state, was successfully predicted, whereas the  $\sigma$  meson, a long-term candidate for a non-ordinary meson, was found to follow a completely different trajectory.

In the first part of this work we have successfully predicted the trajectories of the other two, well-established ordinary resonances, the  $f_2(1270)$  and  $f_2'(1525)$ . In particular, from parameters of the associated poles in the complex energy plane we have calculated their trajectories and have shown that they are almost real and very close to a straight line, as expected.

In the second part of this work we have addressed the question of whether choosing two subtractions in dispersion relations of [4] was actually imposing that the real part of the trajectory is a straight line for relatively narrow resonances. To address this question we analyzed the same resonances using a dispersion relation with an additional subtraction. We have shown that within the range of applicability of our approach, which basically coincides with the elastic regime, the resulting trajectories are once again very close to a straight line. In the third part we have slightly modified the method to accommodate different masses for the masses of the scattering particles and studied, both with two and three subtractions, the  $K^*(892)$  trajectory obtained from its pole in  $K\pi$  scattering. The resulting trajectory comes out also almost real and linear with the universal slope.

In the future it will be interesting to use such dispersive methods to determine trajectories of other mesons, as long as they are almost elastic, as it is the case of the controversial  $K^*(800)$ , which is another long-time candidate for a non-ordinary meson. Heavy mesons in charm and beauty sectors can also be examined. We also plan to extend the method to meson–baryon scattering, where, for example, the  $\Delta(1232)$  is another candidate for an ordinary resonance. We are also planning on extending the approach to coupled channels.

## Acknowledgements

We would like to thank M.R. Pennington for several discussions. J.R.P. and J.N. are supported by the Spanish project FPA2011-27853-C02-02 and the Spanish network FIS2014-57026-REDT. J.N. acknowledges funding by the Fundación Ramón Areces. A.P.S. work is supported in part by the U.S. Department of Energy, Office of Science, Office of Nuclear Physics under contracts DE-AC05-06OR23177 and DE-FG0287ER40365.

## References

- [1] R.L. Jaffe, *Phys. Rev. D* 15 (1977) 267;

- R.L. Jaffe, Prog. Theor. Phys. Suppl. 168 (2007) 127;  
J.D. Weinstein, N. Isgur, Phys. Rev. Lett. 48 (1982) 659;  
D. Black, A.H. Fariborz, F. Sannino, J. Schechter, Phys. Rev. D 59 (1999) 074026;  
P. Minkowski, W. Ochs, Eur. Phys. J. C 9 (1999) 283;  
J.A. Oller, E. Oset, Nucl. Phys. A 620 (1997) 438;  
J.A. Oller, E. Oset, Nucl. Phys. A 652 (1999) 407 (Erratum);  
E. van Beveren, G. Rupp, Eur. Phys. J. C 22 (2001) 493;  
J.R. Pelaez, Phys. Rev. Lett. 92 (2004) 102001;  
J. Vijande, A. Valcarce, F. Fernandez, B. Silvestre-Brac, Phys. Rev. D 72 (2005) 034025;  
J.R. Pelaez, G. Rios, Phys. Rev. Lett. 97 (2006) 242002;  
F. Giacosa, Phys. Rev. D 74 (2006) 014028;  
J.R. Pelaez, M.R. Pennington, J. Ruiz de Elvira, D.J. Wilson, Phys. Rev. D 84 (2011) 096006;  
T. Hyodo, D. Jido, T. Kunihiro, Nucl. Phys. A 848 (2010) 341.  
[2] A.V. Anisovich, V.V. Anisovich, A.V. Sarantsev, Phys. Rev. D 62 (2000) 051502.  
[3] P. Masjuan, E. Ruiz Arriola, W. Broniowski, Phys. Rev. D 85 (2012) 094006.  
[4] J.T. Londergan, J. Nebreda, J.R. Pelaez, A. Szczepaniak, Phys. Lett. B 729 (2014) 9, arXiv:1311.7552 [hep-ph].  
[5] I. Caprini, G. Colangelo, H. Leutwyler, Phys. Rev. Lett. 96 (2006) 132001, arXiv:hep-ph/0512364;  
R. Garcia-Martin, R. Kaminski, J.R. Pelaez, J. Ruiz de Elvira, Phys. Rev. Lett. 107 (2011) 072001, arXiv:1107.1635 [hep-ph].  
[6] P.B.D. Collins, An Introduction to Regge Theory & High Energy Physics, Cambridge University Press, Cambridge, 1977;  
V.M. Gribov, The Theory of Complex Angular Momenta, Cambridge University Press, Cambridge, 2003.  
[7] P.D.B. Collins, R.C. Johnson, E.J. Squires, Phys. Lett. B 26 (1968) 223.  
[8] G. Epstein, P. Kaus, Phys. Rev. 166 (1968) 1633;  
S.-Y. Chu, G. Epstein, P. Kaus, R.C. Slansky, F. Zachariasen, Phys. Rev. 175 (1968) 2098.  
[9] R. Garcia-Martin, R. Kaminski, J.R. Pelaez, J. Ruiz de Elvira, F.J. Yndurain, Phys. Rev. D 83 (2011) 074004, arXiv:1102.2183 [hep-ph].  
[10] K.A. Olive, et al., Particle Data Group, Chin. Phys. C 38 (2014) 090001.